ACS APPLIED MATERIALS & INTERFACES

Research Article

www.acsami.org

Hollow Metal–Organic Framework Nanospheres via Emulsion-Based Interfacial Synthesis and Their Application in Size-Selective Catalysis

Yufen Yang,[†,‡] Fengwei Wang,[†,‡] Qihao Yang,[§] Yingli Hu,[§] Huan Yan,[∥] Yu-Zhen Chen,[§] Huarong Liu,*[,‡] Guoqing Zhang,[‡] Junling Lu,[∥] Hai-Long Jiang,*[,§] and Hangxun Xu*[,‡]

[‡]CAS Key Laboratory of Soft Matter Chemistry, Department of Polymer Science and Engineering, [§]Department of Chemistry, Hefei National Laboratory for Physical Sciences at the Microscale, and [∥]Department of Chemical Physics, Hefei National Laboratory for Physical Sciences at the Microscale, University of Science and Technology of China, Hefei, Anhui 230026, China

Supporting Information

ABSTRACT: Metal–organic frameworks (MOFs) represent an emerging class of crystalline materials with well-defined pore structures and hold great potentials in a wide range of important applications. The functionality of MOFs can be further extended by integration with other functional materials, e.g., encapsulating metal nanoparticles, to form hybrid materials with novel properties. In spite of various synthetic approaches that have been developed recently, a facile method to prepare hierarchical hollow MOF nanostructures still remains a challenge. Here we describe a facile emulsion-based interfacial reaction method for the large-scale synthesis of hollow zeolitic imidazolate framework 8 (ZIF-8) nanospheres with controllable shell thickness. We further demonstrate that functional metal nanoparticles such as Pd nanocubes can be encapsulated during the emulsification process and used for heterogeneous catalysis. The inherently porous structure of ZIF-8 shells enables encapsulated catalysts to show size-selective hydrogenation reactions.

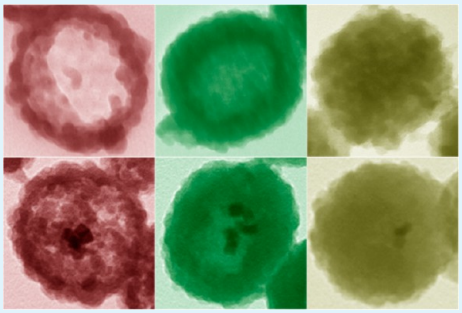

KEYWORDS: *emulsion, hollow nanostructures, interfacial reactions, metal–organic frameworks, catalysis*

INTRODUCTION

Inspired by their diverse and uniform porosity, metal–organic frameworks (MOFs) or porous coordination polymers (PCPs) are very promising for applications in gas storage, separation, drug delivery, sensing, and catalysis.[1−9] They are synthesized based on well-established principles of coordination chemistry via self-assembling of metal ions or clusters with polytopic organic ligands under appropriate conditions. The vast combination of organic ligands with inorganic nodes provides a versatile approach to prepare porous crystals with unique structures and properties.[10−13] Although most studies involving MOFs are based on crystalline solids, recent research has indicated that developing advanced architectures of MOFs could further expand the scope of these materials in many applications and facilitate their integration with other functional materials, thus imparting new functionalities.[14−19]

Recently, much effort has been devoted to preparing MOF superstructures to better exploit the well-defined pore structures of MOFs; especially hollow MOFs with thin shells could exhibit selective permeability for delivery and catalysis purposes.[20,21] So far, several different methods have been reported to prepare hollow MOF structures.[22−28] For example, polymer microspheres and metal oxides were introduced as templates to prepare hollow MOFs, although this preparation strategy involved tedious etching steps.[22−24] New synthetic approaches like microfluidic technique, spray drying, and emulsion-based interfacial assembly have also been developed to prepare hollow MOFs at the micrometer scale.[29−33] Compared to a large number of fabrication methods on the preparation of hollow inorganic materials at the nanoscale,[34−38] constructing nanosized hollow MOFs still remains a big challenge and only a limited number of reports appeared in the literature without involving templates thus far.[26,27] Herein, we show that hollow MOF nanospheres with controllable shell thickness can be obtained using a facile emulsion-based interfacial synthesis. We choose zeolitic imidazolate framework 8 (ZIF-8), which has high thermal and chemical stability as the model system to demonstrate our approach.[39,40]

Emulsion synthesis has been extensively used in the large-scale preparation of latexes and even manufacture of several important commercial polymers.[41−43] Interfacial emulsion polymerization has been extensively used to prepare hollow polymeric nanoparticles.[44,45] Emulsion droplets were also previously used as microreactors to prepare MOF nanocrystals with accelerated reaction rates.[46−48] However, unlike emulsion polymerization and previous MOF preparation using emulsion synthesis, which typically occurs inside the emulsion droplets, here the nucleation and growth of ZIF-8 nanocrystals and their formation of continuous shells takes place at the water/1-octanol interface stabilized by polyvinylpyrrolidone (PVP) at room temperature (Scheme 1). A distinct feature of this method is that we are able to obtain a large quantity of hollow

Received: August 1, 2014
Accepted: September 23, 2014
Published: September 23, 2014

Scheme 1. Schematic Illustration of the Process for the Preparation of Hollow ZIF-8 Nanospheres via an Emulsion-Based Approach[a]

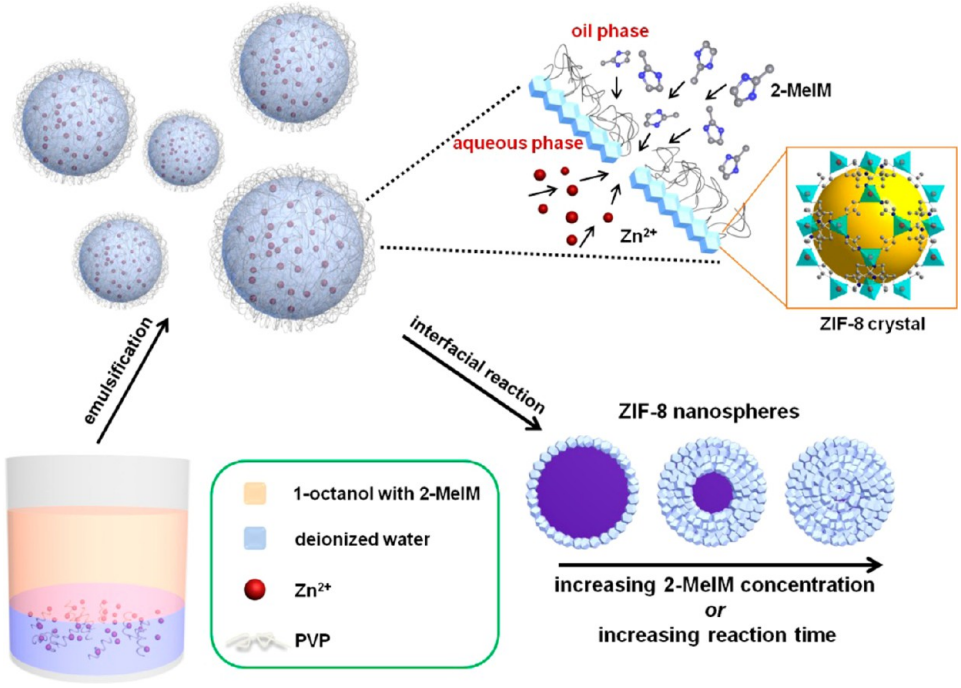

[a]A water-in-oil nanoemulsion can be prepared using PVP as stabilizer and 1-octanol as the oil phase. Zinc ions in the aqueous phase coordinate with 2-MeIM in 1-octanol at the spherical interfaces of emulsion droplets, forming ZIF-8 nanocrystals which further grow to form nanospheres at room temperature. Controlling the concentration of 2-MeIM and reaction time can lead to the formation of hollow ZIF-8 nanospheres with different shell thicknesses.

ZIF-8 nanospheres with high yield, ~50%, as shown in Figure S1 of the Supporting Information. In this approach, the nanosized emulsion droplets act as temporary spherical templates, which can be easily removed during the purification process without etching. In addition, the reactions at the interface of two immiscible liquids exhibit an intrinsically self-completing property so that zinc ions and 2-methylimidazole (2-MeIM) ligands will contact at thinner or defect sites to avoid the formation of cracks and large voids.[29] The shell thickness can be easily controlled by tuning the amount of precursors used or by varying the crystallization time. Furthermore, functional nanomaterials such as Pd nanocubes can be easily encapsulated into the cavities of ZIF-8 nanospheres to form Pd@ZIF-8 nanospheres by introducing Pd nanocubes to the aqueous phase during the emulsification process. Because of the well-defined pore aperture of ZIF-8, only reactants with suitable molecular sizes could pass through the outer shell, which makes them promising candidates in size-selective catalysis.[17,23,24]

RESULTS AND DISCUSSION

The structure and morphology of as-prepared hollow ZIF-8 nanospheres were examined using a transmission electron microscope (TEM) and a scanning electron microscope (SEM). The SEM and TEM images showed that spherical nanospheres with average diameters around 130 nm can be obtained (Figure 1). Obviously, as the concentration of organic ligands increased from 0.76 to 1.52 M, the shell thickness increased from ~20 nm (ZIF-8 (T), T represents thin shell) (Figure S2 in the Supporting Information) to ~50 nm (ZIF-8 (M), M represents medium thickness) while the diameters of ZIF-8 nanospheres were roughly the same. When the concentration further increased to 2.28 M, solid nanospheres (ZIF-8 (S), here S represents solid sphere) instead of hollow structure can be obtained. Varying the reaction time could also lead to the formation of hollow ZIF-8 nanospheres with different shell thicknesses when the concentration of precursors were kept the same. As shown in Figure 2, with the increase of reaction time from 1 to 48 h, the shell thickness could increase from ~15 to ~70 nm. High-magnification TEM images revealed that such prepared ZIF-8 nanospheres consisted of numerous small ZIF-8 nanocrystals. As revealed by powder X-ray diffraction (PXRD) measurements, the resulting nanospheres clearly showed typical sodalite topology of ZIF-8, as evidenced by good agreement with the simulated results (Figure 3). Peak broadening can be observed from the sample PXRD patterns, indicating the formation of nanosized ZIF-8 crystals, which is consistent with TEM observation. The average crystallite sizes calculated from the Scherrer equation are around 20 nm, which is consistent with the observation from TEM images.

The progress of an interfacial reaction highly depends on the dispersive behaviors of reactants in the separated two phases which could control the diffusion of reactants from one phase to the other phase.[29,30,49,50] In this emulsion-based interfacial synthesis, Zn^{2+} were confined in the aqueous phase and 2-MeIM were dispersed in the 1-octanol phase. As ZIF-8 nanocrystals started nucleation at the interface, they generated a hydrophobic environment which could facilitate the diffusion of 2-MeIM from the 1-octanol phase to the interface and further toward the aqueous phase due to the hydrophobic nature of ZIF-8.[39,51] Therefore, ZIF-8 nanocrystals continued to grow inward to form hollow nanospheres with controlled

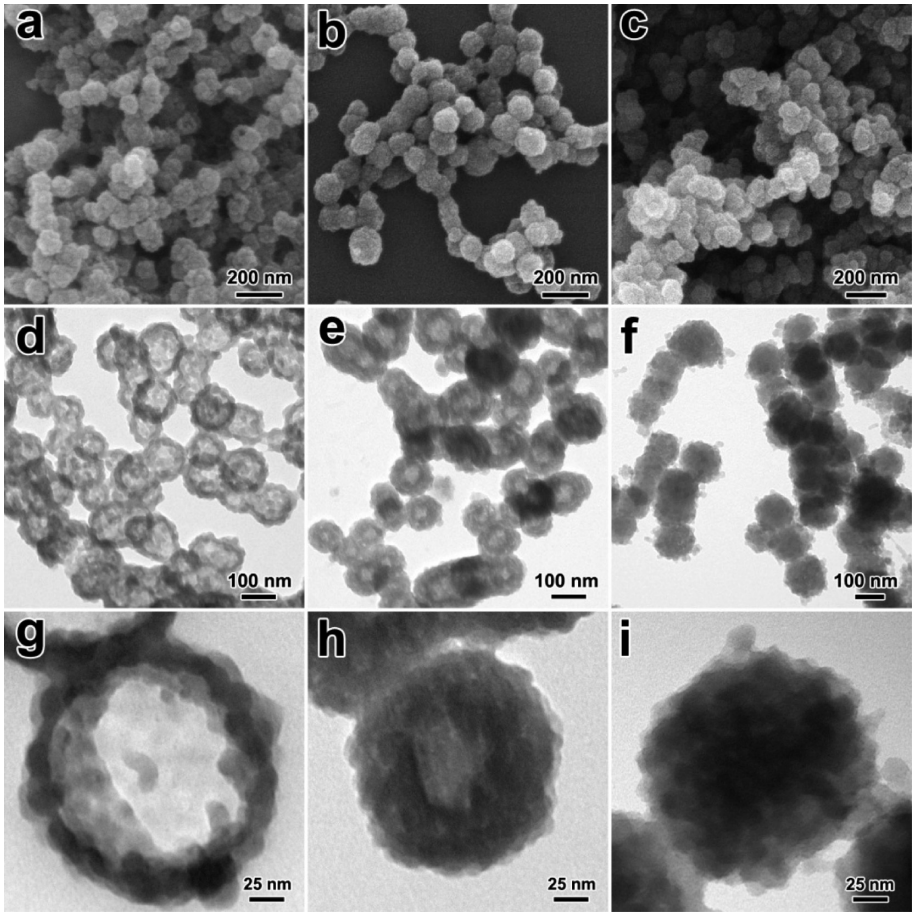

Figure 1. SEM (a–c) and TEM (d–i) images of hollow ZIF-8 nanospheres obtained with different concentrations of 2-MeIM while the amount of Zn^{2+} is constant (the concentration of Zn^{2+} is 0.15 M): (a,d,g) 0.76 M, (b,e,h) 1.52 M, and (c,f,i) 2.28 M.

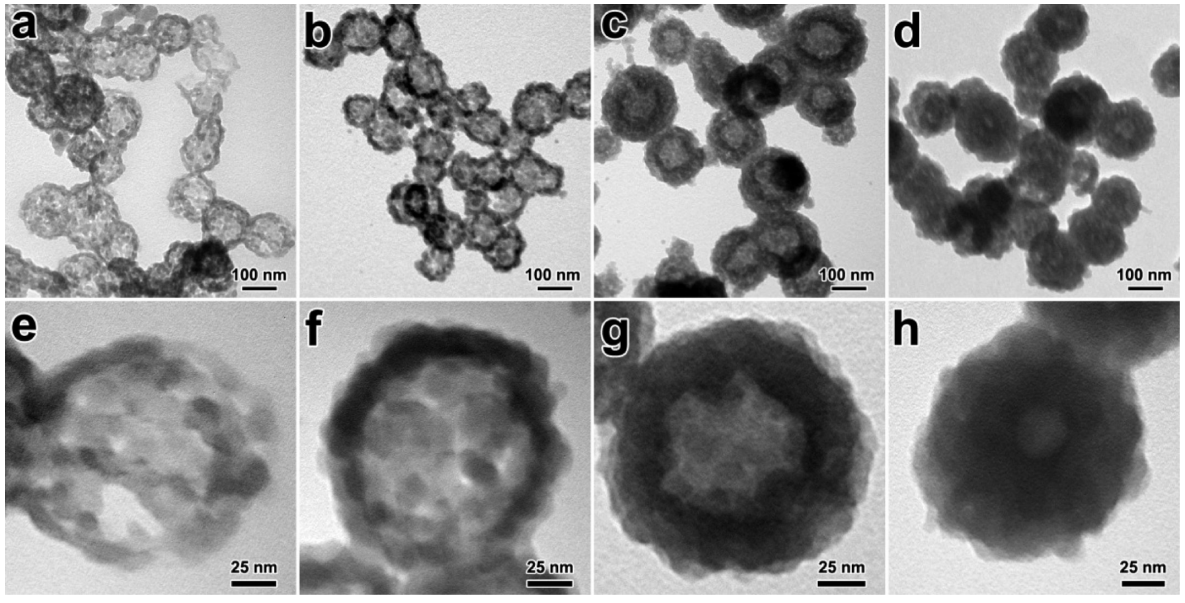

Figure 2. TEM images of hollow ZIF-8 nanospheres obtained by controlling the reaction time (the concentrations of Zn^{2+} and 2-MeIM are 0.15 and 1.52 M, respectively): (a,e) 1 h, (b,f) 3 h, (c,g) 6 h, and (d,h) 48 h.

shell thickness while the size of the nanospheres remained the same. We could also extend this synthetic route to prepare other hollow MOF nanospheres such as HKUST-1. As shown in Figure S3 of the Supporting Information, hollow HKUST-1 nanospheres were obtained at very short reaction time (~10 min) and solid HKUST-1 nanospheres were formed in 30 min. Compared to ZIF-8, the formation of HKUST-1 nanospheres is much faster, which is likely due to the fast diffusion of trimesic

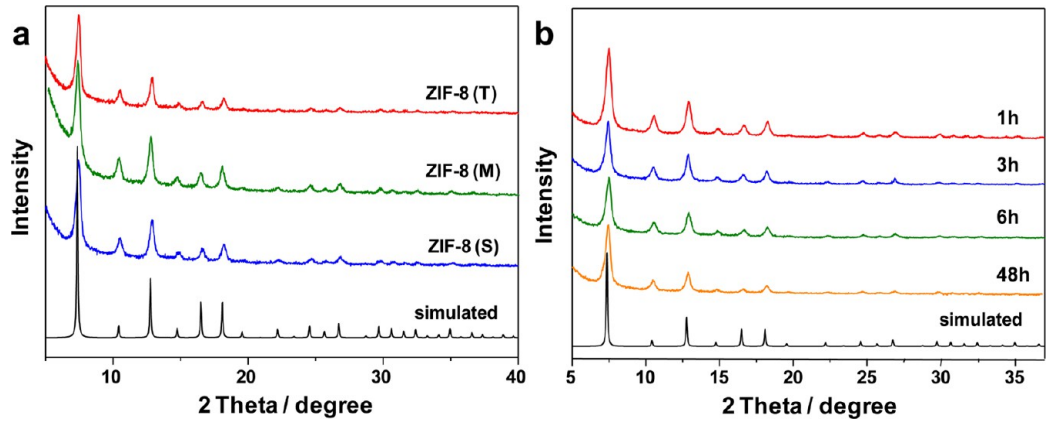

Figure 3. Powder XRD patterns of hollow ZIF-8 nanospheres prepared using different concentrations of 2-MeIM (a) and different reaction times (b).

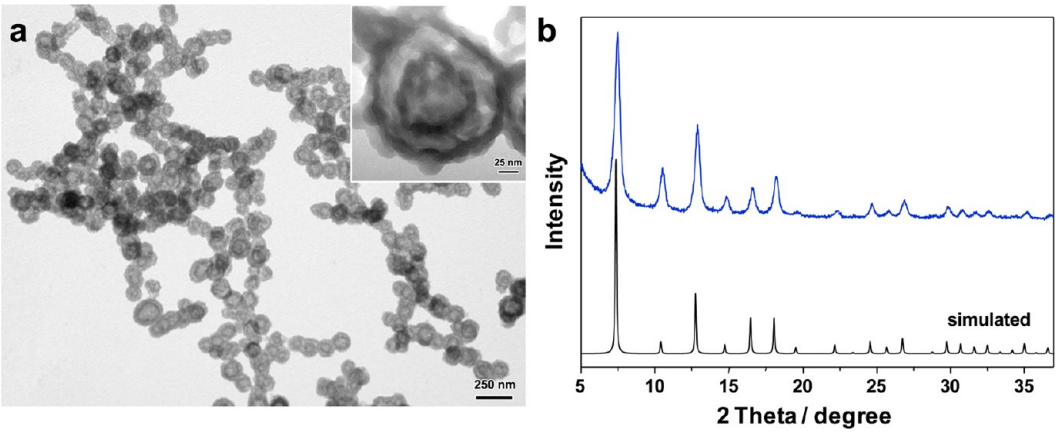

Figure 4. (a) TEM images of double-shell hollow ZIF-8 nanospheres obtained using this emulsion approach (inset shows a single magnified nanosphere). (b) Powder XRD pattern of double-shell hollow ZIF-8 nanospheres as shown in (a).

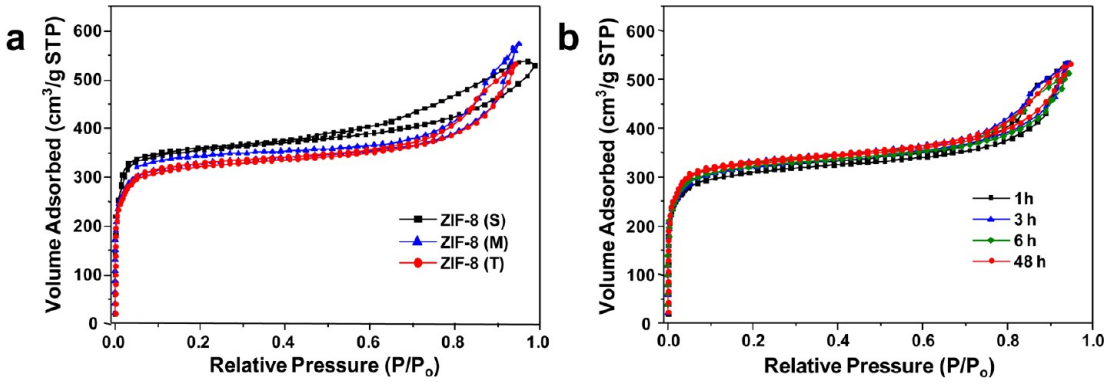

Figure 5. Nitrogen adsorption−desorption isotherms of hollow ZIF-8 nanospheres obtained with different concentrations of 2-MeIM (a) and different reaction times (b).

acid from oil phase to aqueous phase as trimesic acids contain three highly hydrophilic carboxylic groups.

We also examined the effect of Zn^{2+} on the formation of ZIF-8 nanospheres while keeping the concentration of 2-MeIM constant (1.52 M). Hollow spherical structures could not be obtained at low Zn^{2+} concentrations (0.038 and 0.076 M), and instead, only noncontinuous networks and broken spheres with thin shells can be found (Figure S4 of the Supporting Information). When Zn^{2+} increased to 0.092 M (Figure S4 of the Supporting Information), hollow nanospheres with loose porous structure can be obtained. Increasing the Zn^{2+} to 0.15 M lead to the formation of hollow nanospheres with thick shells similar to that of Figure 1e. Surprisingly, when the concentration of Zn^{2+} was adjusted to 0.11 M, which was slightly lower than that to form dense hollow nanospheres, double-shell hollow ZIF-8 nanospheres emerged (Figure 4a). These double-shell nanospheres exhibited diffraction pattern identical to that of ZIF-8 crystals (Figure 4b).

Double-shell nanostructures are usually prepared involving multiple templating and etching steps.[52,53] In our method,

however, neither exotemplate nor multiple growth was involved. The nucleation and formation of ZIF-8 nanocrystals first took place at the interface between the aqueous phase and the 1-octanol phase, leading to the formation of a thin layer of ZIF-8. As the reaction proceeded and because of the hydrophobic nature of ZIF-8 layer, 2-MeIM can diffuse inward to coordinate with Zn^{2+} to form new ZIF-8 nanocrystals. If a large amount of Zn^{2+} was added into the aqueous phase, besides the first layer of ZIF-8 nanocrystals formed at the liquid−liquid interface, more ZIF-8 layers can gradually grow and eventually lead to the formation of hollow nanospheres as shown in Figures 1 and 2 (Scheme 1). If inadequate Zn^{2+} are present in the aqueous phase, they were not sufficient to form enough ZIF-8 nanocrystals to afford integral shells. Therefore, only loose and noncontinuous networks of ZIF-8 nanocrystals were obtained (Figure S4 of the Supporting Information). When a moderate amount of Zn^{2+} was used, ZIF-8 nanocrystals can initially grow at the interface to form a thin shell. As the reaction proceeds, excess 2-MeIM could diffuse inward the aqueous phase to react with remaining Zn^{2+} to generate new ZIF-8 nanocrystals next to the first layer (Figure S5a of the Supporting Information). In this case, however, Zn^{2+} in the aqueous phase were mostly depleted as the reaction proceeded. Therefore, an Ostwald ripening process occurred between the initial shell and the newly formed ZIF-8 layer to form a small gap (Figure S5b of the Supporting Information), which reacted further to give a large gap and eventually lead to the formation of the double-shell structure.[25]

The permanent porosity of hollow ZIF-8 nanospheres prepared via emulsion-based interfacial synthesis was confirmed by nitrogen-sorption measurements. As shown in Figure 5, type-IV isotherms were observed for all ZIF-8 nanospheres. The steep increases in N_2 uptake at a low relative pressure ($\leq$0.01), as does ZIF-8, indicate the microporosity. The appearance of the asymmetric hysteresis loops might be caused by the existence of mesopores corresponding to the central cavities and inevitable voids between neighboring ZIF-8 nanocrystals. The Brunauer−Emmett−Teller (BET) surface areas of hollow ZIF-8 nanospheres obtained with increasing concentrations of 2-MeIM were 984, 1011, and 1098 m^2/g, respectively. This slight increase might be caused by the formation of more mesopores and/or micropores between adjacent ZIF-8 nanocrystals as the concentration of precursors and reaction time increased. Hollow ZIF-8 nanospheres prepared in this interfacial synthesis exhibited lower surface areas compared to ZIF-8 crystals obtained by conventional solvothermal method, which could be ascribed to the lower synthetic temperature used in this method.[54]

Thermal degradation investigations indicated that hollow ZIF-8 nanospheres start decomposing in air at a temperature around 300 °C (Figure S6 of the Supporting Information). After thermal decomposition, approximately 35% of the starting weight remained, corresponding to the formation of zinc oxide. FT-IR spectra of hollow ZIF-8 nanospheres exhibited no dramatic difference as compared to that of pure ZIF-8 crystals (Figure S7 of the Supporting Information), indicating great chemical purity of such prepared hollow ZIF-8 nanospheres. In addition, the characteristic peak at 1660 cm^{-1} corresponding to the stretching vibration of C═O groups in PVP disappeared in all hollow ZIF-8 nanospheres. The absence of such peaks in all obtained ZIF-8 nanospheres indicates that all polymeric stabilizers initially covering the emulsion droplets were completely removed during the post-treatment process.

This facile emulsion-based interfacial synthesis not only can generate hollow MOF nanostructures but also is able to encapsulate functional nanoparticles into hollow nanospheres simultaneously. Nanoparticles encapsulated in MOF composites are usually prepared by the reduction of metal precursors inside the MOF channels, or by in situ templating presynthesized nanoparticles in the MOF growth solutions.[17−19,55−59] In our approach, the water-soluble functional nanomaterials could be first introduced into aqueous phase and subsequent emulsion process would confine nanomaterials inside aqueous droplets. Using this method, yolk−shell or core−shell nanospheres can be obtained depending on the synthetic conditions. In this work, we chose Pd nanocubes which show excellent catalytic performance for encapsulation study, although this approach can be extended to afford other functional materials. As shown in Figure 6, the addition of

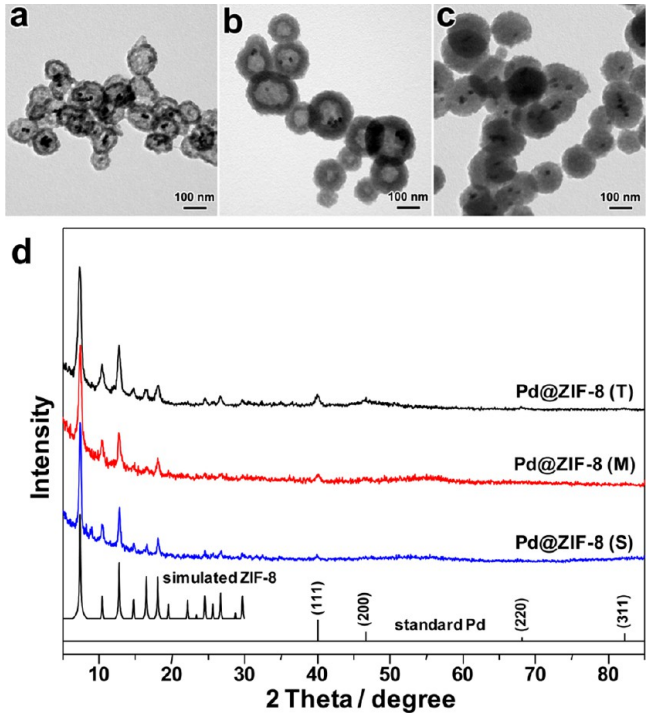

Figure 6. TEM images of ZIF-8 nanospheres encapsulated with Pd nanocubes: (a) Pd@ZIF-8 (T), (b) Pd@ZIF-8 (M), and (c) Pd@ZIF-8 (S). (d) Powder XRD patterns of Pd@ZIF-8 nanospheres obtained using this emulsion-based synthesis.

presynthesized PVP-stabilized Pd nanocubes (Figure S8 of the Supporting Information) into the reaction system could yield yolk−shell and core−shell Pd@ZIF-8 nanospheres when the same synthetic conditions as that of Figure 1 were employed. PXRD patterns of Pd@ZIF-8 nanospheres revealed that the encapsulation process essentially had no influence on the formation of the ZIF-8 nanocrystals (Figure 6d). Inductively coupled plasma (ICP) analysis indicated that the Pd content varied with different ZIF-8 nanostructures. When Pd nanocubes were equally introduced into ZIF-8 nanospheres, Pd@ZIF-8 (T) showed the highest loading amount with 4.59% and this number decreased to 3.18% and 1.94% for Pd@ZIF-8 (M) and Pd@ZIF-8 (S), respectively. This is consistent with the observation that the average weight of ZIF-8 nanospheres increased from ZIF-8 (T) to ZIF-8 (S) as their structures evolved from hollow to solid. Compared to strong diffraction

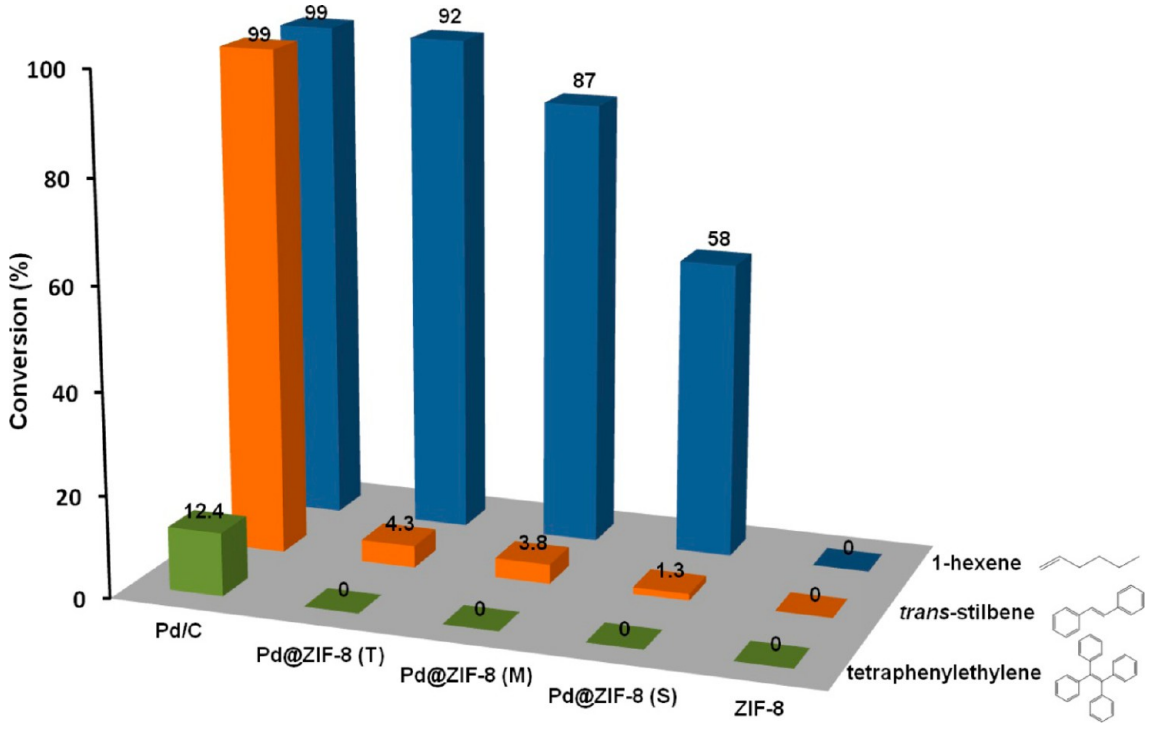

Figure 7. Catalytic performance of Pd@ZIF-8 nanospheres for the liquid-phase hydrogenation of 1-hexene, *trans*-stilbene, and tetraphenylethylene with different ZIF-8 shell thicknesses. Pure ZIF-8 and Pd/C (Pd content 5%) were used as controls.

peaks that originate from ZIF-8 nanocrystals, peaks associated with Pd nanocubes within nanospheres were indiscernible and only a prominent peak at (111) could be detected for the face-centered cubic Pd nanocores (JCPDS No. 05-0681), presumably because of their low loading amount.[18] The N_2 adsorption−desorption isotherms of Pd@ZIF-8 nanospheres also displayed type-IV isotherms, which are similar to those of ZIF-8 nanospheres without Pd nanocubes (Figure S9 of the Supporting Information). Compared to ZIF-8 nanospheres without Pd nanocubes, the Pd@ZIF-8 nanospheres showed slightly lower BET surface areas which could be accounted for by the encapsulation of heavy and nonporous Pd nanocubes.

This approach can efficiently confine all presynthesized Pd nanocubes within the framework material and the encapsulation efficiency is nearly 100%. Therefore, the well-defined pore structure of MOF shells can be used as molecular sieves for selective catalysis. As a proof of concept, liquid-phase hydrogenation of olefins with different molecular sizes was chosen as a model reaction to demonstrate the structural advantage of these Pd@ZIF-8 nanospheres in selective catalysis. For this purpose, 1-hexene, *trans*-stilbene, and tetraphenylethylene were chosen for hydrogenation probe reactions. As shown in Figure 7, Pd@ZIF-8 nanospheres with different shell thicknesses display different conversion rates for olefins with different molecular sizes. For 1-hexene, yolk−shell Pd@ZIF-8 nanospheres with thin ZIF-8 layer showed the highest activity with 98% conversion after 24 h reaction, indicating that thin ZIF-8 shell has negligible influence on the diffusion of 1-hexene molecules (molecular size ∼2.5 Å, kinetic diameter ∼4.3 Å). The conversion rate decreased to 87% when yolk−shell Pd@ZIF-8 nanospheres with thicker shell were used as catalysts. In contrast, core−shell Pd@ZIF-8 nanospheres only showed 58% conversion during the same reaction period, presumably because of a lower diffusion rate through a much thicker ZIF-8 shell in this structure, and the decreased Pd reaction sites which are partially blocked by ZIF-8 nanocrystals. *trans*-Stilbene has a much larger molecular size (5.6 Å) than the pore aperture of ZIF-8 (3.4 Å) and therefore they cannot move freely through the ZIF-8 shells and can only diffuse through the limited mesoporous voids between ZIF-8 nanocrystals in the shells (Figure S9 of the Supporting Information). Accordingly, the conversion rates decreased to 4.3−1.3% and the yield reasonably lower along with thicker ZIF-8 shell. When it comes to molecules with even larger size such as tetraphenylethylene (6.7 Å), Pd@ZIF-8 nanospheres showed no activity to hydrogenation reaction (Figure S10 of the Supporting Information). This observation also suggests that all Pd nanocubes are confined in the ZIF-8 shells, which is consistent with TEM observation. In the control experiment, pure ZIF-8 nanocrystals showed no catalytic activity toward all unsaturated compounds. Pd supported on carbon displayed the same conversion rate for 1-hexene and *trans*-stilbene (99%) and a much lower conversion rate for tetraphenylethylene (12%). It is likely that the four phenyl groups in tetraphenylethylene make it difficult for carbon double bonds to contact catalytically active sites on the Pd surface.[18] Furthermore, because all Pd nanocubes are protected by a layer of ZIF-8 shell, they can be recycled for multiple consecutive catalytic reactions. In the case of hydrogenation of 1-hexene, even after three cycles of consecutive runs, the Pd@ZIF-8 (T) nanospheres still exhibited very high conversion efficiency and also unaltered nanostructure (Figure S11 of the Supporting Information). Meanwhile, powder XRD measurements indicated that the sodalite topology of ZIF-8 were well preserved (Figure S12 of the Supporting Information).

CONCLUSION

In conclusion, we demonstrated that emulsion-based interfacial reactions can be conveniently used for the large-scale

preparation of hollow MOF nanospheres. Instead of using emulsion droplets as microreactors for the formation of nanosized MOFs, nanodroplets formed during the emulsification process can act as temporary templates for the formation of hollow MOF nanostructures with well controllable shell thickness. Furthermore, we also successfully encapsulated functional metal nanoparticles into the cavity of hollow MOFs simply by introducing presynthesized nanomaterials during the emulsification process. This encapsulation strategy ensures that nanoparticles are completely confined within the MOF shells without altering their porous structures. With active nanoparticles inside the cavity, the outer MOF shell not only can be used as a molecular sieve for size-selective catalysis but also can serve as a protection layer to prevent functional nanoparticles from aggregation during the reactions so as to maintain the catalytic activity. Given the vast selection of both MOFs and nanomaterials, such a general emulsion-based interfacial approach to hollow MOF nanostructures would have great potential and opens a new avenue to MOF nanocomposites incorporating various nanomaterials in non-agglomerated fashion with predesigned functionalities.

EXPERIMENTAL SECTION

Materials. Zinc acetate dihydrate (98%), 2-methylimidazole (99%), trimesic acid (98%), L-ascorbic acid (99%), copper nitrate trihydrate, potassium bromide (99%), potassium tetrachloropalladate (98%), and 1-octanol (99%) were purchased from Sigma-Aldrich and used without purification. Polyvinylpyrrolidone (PVP, average M_w = 24 000, K_{23-27}) was purchased from Aladdin Reagents and used as received.

Synthesis of Hollow ZIF-8 Nanospheres. We conducted the synthesis with many different concentrations of Zn^{2+} and 2-MeIM. Generally, the aqueous phase was prepared by dissolving a certain amount of zinc acetate dihydrate to deionized (DI) water containing 3.8 wt % PVP. The oil phase was prepared by dissolving different amounts of 2-MeIM into 1-octanol to form stable solutions. Then the aqueous solution was added into 1-octanol and stirred/vortexed to obtain a stable inverse emulsion. Next, the organic−ligand solution was added to the above emulsion and gently shaken for a few seconds to initiate interfacial reaction. The samples were kept without perturbation at room temperature for a certain time and subsequently centrifuged to collect final products. For example, for the synthesis of hollow ZIF-8 nanospheres with thin shells (ZIF-8 (T)), 13 mg of zinc acetate dihydrate was added into 0.4 mL of DI water containing 16 mg of PVP. The aqueous solution was added into 24 mL of 1-octanol and vortexed to generate a stable inverse emulsion. Then 6 mL of 1-octanol solution containing 375 mg of 2-MeIM was added to the emulsion to initiate the reaction. The above solution was kept without perturbation at room temperature for 24 h before purification. The obtained samples were further washed with methanol several times and dried overnight in the vacuum oven.

Synthesis of PVP-Capped Pd Nanocubes. Eight milliliters of an aqueous solution containing 105 mg of PVP, 60 mg of L-ascorbic acid, and 600 mg of KBr was added into a 20 mL vial. The solution was preheated under magnetic stirring at 80 °C for 15 min. Next, 3 mL of another aqueous solution dissolving 57 mg of K_2PdCl_4 was added using a pipet. The reaction proceeded at 80 °C for 3 h. The products were collected by centrifugation and washed three times with water to remove excess PVP.

Synthesis of Pd@ZIF-8 Nanospheres. The preparation process was exactly the same as that for the preparation of corresponding ZIF-8 nanospheres unless presynthesized PVP-stabilized Pd nanocubes were added into the aqueous phase during the emulsification process. Interfacial reaction proceeded at room temperature for 24 h and centrifuged to collect ZIF-8 nanospheres encapsulated with Pd nanocubes. The obtained samples were further washed with methanol several times and dried overnight in the vacuum oven.

General Procedures for Liquid-Phase Hydrogenation Reactions. The selective hydrogenation of olefins (1-hexene, *trans*-stilbene, or 1,1,2,2-tetraphenylethylene, all purchased from Sigma-Aldrich) was carried out in batch mode at a pressure of 1 bar static hydrogen, at a concentration of 1.93 mmol of olefin/mg of Pd. In a typical experiment, the catalyst was loaded in a reactor and the residual air in the reactor was expelled by flushing hydrogen several times. Ethyl acetate (1.5 mL) was added in the reactor and the mixture was stirred for 5 min to afford a homogeneous suspension. Olefin (0.4 mmol) was then added into the reactor and the mixture was stirred again for 5 min. Then the reactor was again flushed one more time with hydrogen, and the reaction was allowed to proceed at 1 atm of hydrogen and 308 K for 24 h. After the reaction, the catalyst powder was filtered off and the filtrate (1-hexene and *trans*-stilbene) was analyzed and identified by gas chromatography (GC, Shimadzu 2010 Plus with a 0.25 mm × 30 m Rtx-5 capillary column). The catalytic hydrogenation of 1,1,2,2-tetraphenylethylene was monitored using ^{1}H NMR spectrometer (Bruker Avance III 400).

Characterization. Transmission electron microscopy (TEM) and field-emission scanning electron microscopy (FESEM) images were observed on an Hitachi Model H-7560 and JEOL JSM-6700 microscope, respectively. High-resolution TEM was conducted on a JEOL-2010 transmission electron microscope. Thermogravimetric analysis (TGA) was performed on a Shimadzu TGA-50H instrument under air and samples were heated from room temperature to 700 °C at 10 °C/min^{-1}. Powder X-ray diffraction patterns (PXRD) of the product were obtained on a Japan Rigaku DMax-γA rotation anode X-ray diffractometer equipped with graphite monochromatized Cu Kα radiation (λ = 1.54178 Å). The N_2 adsorption−desorption was carried out using Micromeritics ASAP 2020. Prior to the measurements, samples were degassed at 300 °C for 10 h. Fourier transform infrared spectra (FT-IR) were recorded by a VECTOR-22 FT-IR spectrometer over potassium bromide pellet. Inductively coupled plasma mass spectra (ICP-MS) were obtained using Thermo scientific VG PlasmaQuad 3.

ASSOCIATED CONTENT

Supporting Information

Additional TEM, TGA, and FT-IR results of hollow ZIF-8 nanospheres, TEM and PXRD characterization of HKUST-1 nanospheres, TEM and PXRD characterization of as-synthesized Pd nanocubes, nitrogen-sorption measurements of Pd@ZIF-8 nanospheres, and TEM and PXRD of recycled Pd@ZIF-8 nanosphere catalysts. This material is available free of charge via the Internet at http://pubs.acs.org.

AUTHOR INFORMATION

Corresponding Authors

*E-mail: hrliu@ustc.edu.cn.

*E-mail: jianglab@ustc.edu.cn.

*E-mail: hxu@ustc.edu.cn.

Author Contributions

†These authors contributed equally to this work.

Notes

The authors declare no competing financial interest.

■ ACKNOWLEDGMENTS

This work is supported by the National Natural Science Foundation of China (Grant No. 21074122, 51373160, 50873096, 21371162, and 51301159) and the National Key Basic Research Program of China (2014CB931803).

■ REFERENCES

(1) Furukawa, H.; Cordova, K. E.; O'Keeffe, M.; Yaghi, O. M. The Chemistry and Applications of Metal-Organic Frameworks. *Science* **2010**, *341*, 1230444.

(2) Kreno, L. E.; Leong, K.; Farha, O. K.; Allendorf, A.; Van Duyne, R. P.; Hupp, J. T. Metal Organic Framework Materials as Chemical Sensors. *Chem. Rev.* **2012**, *112*, 1105−1125.

(3) Li, J. R.; Sculley, J.; Zhou, H. C. Metal-Organic Frameworks for Separations. *Chem. Rev.* **2012**, *112*, 869−932.

(4) Rocca, J. D.; Liu, D.; Lin, W. Nanoscale Metal-Organic Frameworks for Biomedical Imaging and Drug Delivery. *Acc. Chem. Res.* **2011**, *44*, 957−968.

(5) Aijaz, A.; Xu, Q. Catalysis with Metal Nanoparticles Immobilized within the Pores of Metal-Organic Frameworks. *J. Phys. Chem. Lett.* **2014**, *5*, 1400−1411.

(6) Farrusseng, D.; Aguado, S.; Pinel, C. Metal-Organic Frameworks: Opportunities for Catalysis. *Angew. Chem., Int. Ed.* **2009**, *48*, 7502−7513.

(7) de Voorde, B. V.; Bueken, B.; Denayer, J.; De Vos, D. Adsorptive Separation on Metal-Organic Frameworks in the Liquid Phase. *Chem. Soc. Rev.* **2014**, *43*, 5766−5788.

(8) Cui, Y.; Yue, Y.; Qian, G.; Chen, B. Luminescent Functional Metal-Organic Frameworks. *Chem. Rev.* **2012**, *112*, 1126−1162.

(9) Dhakshinamoorthy, A.; Garcia, H. Catalysis by Metal Nanoparticles Embedded on Metal-Organic Frameworks. *Chem. Soc. Rev.* **2012**, *41*, 5262−5284.

(10) Yaghi, O. M.; O'Keeffe, M.; Ockwig, N. W.; Chae, H. K.; Eddaudi, M.; Kim, J. Reticular Synthesis and the Design of New Materials. *Nature* **2003**, *423*, 705−714.

(11) Kitagawa, S.; Kitaura, R.; Noro, S. Functional Porous Coordination Polymers. *Angew. Chem., Int. Ed.* **2004**, *43*, 2334−2375.

(12) Zhao, D.; Timmons, D. J.; Yuan, D.; Zhou, H. C. Tuning the Topology and Functionality of Metal-Organic Frameworks by Ligand Design. *Acc. Chem. Res.* **2011**, *44*, 123−133.

(13) Guillerm, V.; Kim, D.; Eubank, J. F.; Luebke, R.; Liu, X.; Adil, K.; Lah, M. S.; Eddaoudi, M. A Supermolecular Building Approach for the Design and Construction of Metal-Organic Frameworks. *Chem. Soc. Rev.* **2014**, *43*, 6141−6172.

(14) Foo, M. L.; Matsuda, R.; Kitagawa, S. Functional Hybrid Porous Coordination Polymers. *Chem. Mater.* **2014**, *26*, 310−322.

(15) Doherty, C. M.; Buso, D.; Hill, A. J.; Furukawa, S.; Kitagawa, S.; Falcaro, P. Using Functional Nano- and Microparticles for the Preparation of Metal-Organic Framework Composites with Novel Properties. *Acc. Chem. Res.* **2014**, *47*, 396−405.

(16) Zhu, Q. L.; Xu, Q. Metal-Organic Framework Composites. *Chem. Soc. Rev.* **2014**, *43*, 5468−5512.

(17) Lu, G.; Li, S.; Guo, Z.; Farha, O. K.; Hauser, B. G.; Qi, X.; Wang, Y.; Wang, X.; Han, S.; Liu, X.; DuChene, J. S.; Zhang, H.; Zhang, Q.; Chen, X.; Ma, J.; Loo, S. C. J.; Wei, W.; Yang, Y.; Hupp, J. T.; Huo, F. Imparting Functionality to A Metal-Organic Framework Material by Controlled Nanoparticle Encapsulation. *Nat. Chem.* **2012**, *4*, 310−316.

(18) Zhang, W.; Lu, G.; Cui, C.; Liu, Y.; Li, S.; Yan, W.; Xing, C.; Chi, Y. R.; Yang, Y.; Huo, F. A Family of Metal-Organic Frameworks Exhibiting Size-Selective Catalysis with Encapsulated Noble-Metal Nanoparticles. *Adv. Mater.* **2014**, *26*, 4056−4060.

(19) Meilikhov, M.; Yusenko, K.; Esken, D.; Turner, S.; Van Tendeloo, G.; Fisher, R. A. Metals@MOFs-Loading MOFs with Metal Nanoparticles for Hybrid Functions. *Eur. J. Inorg. Chem.* **2010**, 3701−3714.

(20) Carne-Sanchez, A.; Imaz, I.; Stylianou, K. C.; Maspoch, D. Metal-Organic Frameworks: From Molecules/Metal Ions to Crystals to Superstructures. *Chem.—Eur. J.* **2014**, *20*, 5192−5201.

(21) Furukawa, S.; Reboul, J.; Diring, S.; Sumida, K.; Kiagawa, S. Structuring of Metal-Organic Frameworks at The Mesoscopic/Macroscopic Scale. *Chem. Soc. Rev.* **2014**, *43*, 5700−5734.

(22) Lee, J.; Cho, W.; Oh, M. Advanced Fabrication of Metal-Organic Frameworks: Template-Directed Formation of Polystyrene@ZIF-8 Core-Shell and Hollow ZIF-8 Microspheres. *Chem. Commun.* **2012**, *48*, 221−223.

(23) Kuo, C. H.; Tang, Y.; Chou, L. Y.; Sneed, B. T.; Brodsky, C. N.; Zhao, Z.; Tsung, C. K. Yolk-Shell Nanocrystals@ZIF-8 Nanostructures for Gas-Phase Heterogeneous Catalysis with Selectivity Control. *J. Am. Chem. Soc.* **2012**, *134*, 14345−14348.

(24) Liu, Y.; Zhang, W.; Li, S.; Cui, C.; Wu, J.; Chen, H.; Huo, F. Designable Yolk-Shell Nanoparticle@MOF Petalous Heterostructures. *Chem. Mater.* **2014**, *26*, 1119−1125.

(25) Huo, J.; Wang, L.; Irran, E.; Yu, H.; Gao, J.; Fan, D.; Li, B.; Wang, J.; Ding, W.; Muhammad, A.; Li, C.; Ma, L. Hollow Ferrocenyl Coordination Polymer Microspheres with Micropores in Shells Prepared by Ostwald Ripening. *Angew. Chem., Int. Ed.* **2010**, *49*, 9237−9241.

(26) Hu, M.; Furukawa, S.; Ohtani, R.; Sukegawa, H.; Nemoto, Y.; Reboul, J.; Kitagawa, S.; Yamauchi, Y. Synthesis of Prussian Blue Nanoparticles with a Hollow Interior by Controlled Chemical Etching. *Angew. Chem., Int. Ed.* **2012**, *51*, 984−988.

(27) Zhang, Z.; Chen, Y.; Xu, X.; Zhang, J.; Xiang, G.; He, W.; Wang, X. Well-Defined Metal-Organic Framework Hollow Nanocages. *Angew. Chem., Int. Ed.* **2014**, *53*, 429−433.

(28) Zhang, L.; Wu, H. B.; Lou, X. W. Metal-Organic-Frameworks-Derived General Formation of Hollow Structures with High Complexity. *J. Am. Chem. Soc.* **2013**, *135*, 10664−10672.

(29) Ameloot, R.; Vermoortele, F.; Vanhove, W.; Roeffaers, M. B. J.; Sels, B. F.; De Vos, D. E. Interfacial Synthesis of Hollow Metal-Organic Framework Capsules Demonstrating Selective Permeability. *Nat. Chem.* **2011**, *3*, 382−387.

(30) Brown, A. J.; Brunelli, N. A.; Eum, K.; Rashidi, F.; Johnson, J. R.; Koros, W. J.; Jones, C. W.; Nair, S. Interfacial Microfluidic Processing of Metal-Organic Framework Hollow Fiber Membranes. *Science* **2014**, *345*, 72−75.

(31) Carne-Sanchez, A.; Imaz, I.; Cano-Sarabia, M.; Maspoch, D. A Spray-Drying Strategy for Synthesis of Nanoscale Metal-Organic Frameworks and Their Assembly into Hollow Superstructures. *Nat. Chem.* **2013**, *5*, 203−211.

(32) Pang, M.; Cairns, A. J.; Liu, Y.; Belmabkhout, Y.; Zeng, H. C.; Eddaoudi, M. Synthesis and Integration of Fe-soc-MOF Cubes into Colloidosomes via a Single-Step Emulsion-Based Approach. *J. Am. Chem. Soc.* **2013**, *135*, 10234−10237.

(33) Huo, J.; Marcello, M.; Garai, A.; Bardshaw, D. MOF-Polymer Composite Microcapsules Derived from Pickering Emulsions. *Adv. Mater.* **2013**, *25*, 2717−2722.

(34) Zhang, L.; Wu, H.; Madhavi, S.; Hng, H.; Lou, X. W. Formation of Fe_2O_3 Microboxes with Hierarchical Shell Structures from Metal-Organic Frameworks and Their Lithium Storage Properties. *J. Am. Chem. Soc.* **2012**, *134*, 17388−17391.

(35) Hung, L. I.; Tsung, C. K.; Huang, W.; Yang, P. Room-Temperature Formation of Hollow Cu_2O Nanoparticles. *Adv. Mater.* **2010**, *22*, 1910−1914.

(36) Yin, Y. D.; Rioux, R. M.; Erdonmez, C. K.; Hughes, S.; Somorjai, G. A.; Alivisatos, A. P. Formation of Hollow Nanocrystals Through the Nanoscale Kirkendall Effect. *Science* **2004**, *304*, 711−714.

(37) Sun, Y.; Mayers, B.; Xia, Y. Metal Nanostructures with Hollow Interiors. *Adv. Mater.* **2003**, *15*, 641−646.

(38) Skrabalak, S. E.; Chen, J. Y.; Sun, Y. G.; Lu, X. M.; Au, L.; Cobley, C. M.; Xia, Y. N. Gold Nanocages: Synthesis, Properties, and Applications. *Acc. Chem. Res.* **2008**, *41*, 1587−1595.
(39) Park, K. S.; Ni, Z.; Cote, A. P.; Choi, J. Y.; Huang, R. D.; Uribe-Romo, F. J.; Chae, H. K.; O'Keeffe, M.; Yaghi, O. M. Exceptional Chemical and Thermal Stability of Zeolitic Imidazolate Frameworks. *Proc. Natl. Acad. Sci. U. S. A.* **2006**, *103*, 10186−10191.
(40) Huang, X. C.; Lin, Y. Y.; Zhang, J. P.; Chen, X. M. Ligand-Directed Strategy for Zeolite-Type Metal-Organic Frameworks: Zinc(II) Imidazolates with Unusual Zeolitic Topologies. *Angew. Chem., Int. Ed.* **2006**, *45*, 1557−1559.
(41) Gutierrez, J. M.; Gonzalez, C.; Maestro, A.; Sole, I.; Pey, C. M.; Nolla, J. Nano-Emulsions: New Applications and Optimization of Their Preparation. *Curr. Opin. Colloid Interface Sci.* **2008**, *13*, 245−251.
(42) Zhang, H.; Cooper, A. I. Synthesis and Applications of Emulsion-Templated Porous Materials. *Soft Matter* **2005**, *1*, 107−113.
(43) Asua, J. M. Emulsion Polymerization: From Fundamental Mechanisms to Process Developments. *J. Polym. Sci., Part A: Polym. Chem.* **2004**, *42*, 1025−1041.
(44) Luo, Y.; Gu, H. A General Strategy for Nano-Encapsulation via Interfacially Confined Living/Controlled Radical Miniemulsion Polymerization. *Macromol. Rapid Commun.* **2006**, *27*, 21−25.
(45) Sun, Z.; Luo, Y. Fabrication of Non-Collapsed Hollow Polymeric Nanoparticles with Shell Thickness in the Order of Ten Nanometres and Anti-Reflection Coatings. *Soft Matter* **2011**, *7*, 871−875.
(46) Tanaka, D.; Henke, A.; Albrecht, K.; Moeller, M.; Nakagawa, K.; Kitagawa, S.; Groll, J. Rapid Preparation of Flexible Porous Coordination Polymer Nanocrystals with Accelerated Guest Adsorption Kinetics. *Nat. Chem.* **2010**, *2*, 410−416.
(47) Rieter, W. J.; Taylor, K. M. L.; An, H.; Lin, W. Nanoscale Metal-Organic Frameworks as Potential Multimodal Contrast Enhancing Agents. *J. Am. Chem. Soc.* **2006**, *128*, 9024−9025.
(48) Vaucher, S.; Fielden, J.; Li, M.; Dujardin, E.; Mann, S. Molecule-Based Magnetic Nanoparticles: Synthesis of Cobalt Hexacyanoferrate, Cobalt Pentacyanonitrosylferrate, and Chromium Hexacyanochromate Coordination Polymers in Water-in-Oil Microemulsions. *Nano Lett.* **2002**, *2*, 225−229.
(49) Makiura, R.; Motoyama, S.; Umemura, Y.; Yamanaka, H.; Sakata, O.; Kitagawa, H. Surface Nano-Architecture of A Metal-Organic Framework. *Nat. Mater.* **2010**, *9*, 565−571.
(50) Tsotsalas, M.; Umemura, A.; Kim, F.; Sakata, Y.; Reboul, J.; Kitagawa, S.; Furukawa, S. Crystal Morphology-Directed Framework Orientation in Porous Coordination Polymer Films and Freestanding Membranes via Langmuir-Blodgettry. *J. Mater. Chem.* **2012**, *22*, 10159−10165.
(51) Zhang, K.; Lively, R. P.; Zhang, C.; Chance, R. R.; Koros, W. J.; Sholl, D. S.; Nair, S. Exploring the Framework Hydrophobicity and Flexibility of ZIF-8: From Biofuel Recovery to Hydrocarbon Separations. *J. Phys. Chem. Lett.* **2013**, *4*, 3618−3622.
(52) Yang, M.; Ma, J.; Zhang, C.; Yang, Z.; Lu, Y. General Synthetic Route toward Functional Hollow Spheres with Double-Shelled Structures. *Angew. Chem., Int. Ed.* **2005**, *44*, 6727−6730.
(53) Zhou, L.; Zhao, D.; Lou, X. W. Double-Shelled $CoMn_2O_4$ Hollow Microcubes as High-Capacity Anodes for Lithium-Ion Batteries. *Adv. Mater.* **2012**, *24*, 745−748.
(54) Pan, Y.; Liu, Y.; Zeng, G.; Zhao, L.; Lai, Z. Rapid Synthesis of Zeolitic Imidazolate Framework-8 (ZIF-8) Nanocrystals in An Aqueous System. *Chem. Commun.* **2011**, *47*, 2071−2073.
(55) Schröter, M. K.; Schmid, R.; Khodeir, L.; Muhler, M.; Tissler, A.; Fischer, R. W.; Fischer, R. A. Metal@MOF: Loading of Highly Porous Coordination Polymers Host Lattices by Metal Organic Chemical Vapor Deposition. *Angew. Chem., Int. Ed.* **2005**, *44*, 6237−6241.
(56) Park, Y. K.; Choi, S. B.; Nam, H. J.; Jung, D. Y.; Ahn, H. C.; Choi, K.; Furukawa, H.; Kim, J. Catalytic Nickel Nanoparticles Embedded in A Mesoporous Metal-Organic Framework. *Chem. Commun.* **2010**, *46*, 3086−3088.
(57) Sugikawa, K.; Furukawa, Y.; Sada, K. SERS-Active MetalOrganic Frameworks Embedding Gold Nanorods. *Chem. Mater.* **2011**, *23*, 3132−3134.
(58) Falcaro, P.; Hill, A. J.; Nairn, K. M.; Jasieniak, J.; Mardel, J. I.; Bastow, T. J.; Mayo, S. C.; Gimona, M.; Gomez, D.; Whitfield, H. J.; Ricco, R.; Patelli, A.; Marmiroli, B.; Amenitsch, H.; Colson, T.; Villanova, L.; Buso, D. A New Method to Position and Functionalize Metal-Organic Framework Crystals. *Nat. Commun.* **2011**, *2*, 237.
(59) Aijaz, A.; Karkamkar, A.; Choi, Y. J.; Tsumori, N.; Ronnebro, E.; Autrey, T.; Shioyama, H.; Xu, Q. Immobilizing Highly Catalytically Active Pt Nanoparticles inside the Pores of Metal-Organic Framework: A Double Solvents Approach. *J. Am. Chem. Soc.* **2012**, *134*, 13926−13929.